

New One-Particle Monte Carlo Method for Nanoscale Device Simulation

S. C. Brugger¹ and A. Schenk^{1,†}

¹Integrated Systems Laboratory, ETH Zurich Gloriastrasse 35, CH-8092 Zürich, Switzerland

[†]Synopsys LLC., Affolternstrasse 52, CH-8050 Zürich, Switzerland

¹e-mail: brugger@iis.ee.ethz.ch, Tel: +41 44 632 2348, Fax +41 44 632 1194

[†]e-mail: schenk@iis.ee.ethz.ch, Tel: +41 44 632 6689, Fax +41 44 632 1194

ABSTRACT

In this paper we present a new one-particle Monte Carlo iteration scheme to self-consistently take into account generation-recombination processes as well as quantum corrections. The basic idea is to couple the Boltzmann transport equation (or the Boltzmann-Wigner equation) not only with the Poisson equation, but also with the continuity equation by using exact transport coefficients from the Monte Carlo simulation in high-field regions and the known analytical transport coefficients in low-field regions. This approach is useful e.g. for the simulation of floating-body effects [1] in nanoscale double- and multi-gate SOI MOSFETs.

Keywords: Monte Carlo, Boltzmann equation, SOI MOSFET, generation-recombination, quantum correction

1 INTRODUCTION

17 years ago F. Venturi et al. published the now well-known one-particle Monte Carlo (OPMC) method [2],[3]. The idea of the method is to find a solution to the Boltzmann transport equation (BTE) coupled with the Poisson equation by alternating OPMC simulations and updates of the electric field. This method has the advantage to be "self-consistent" in the sense that ideally after the iteration the density from the Monte Carlo (MC) simulation and the electric field exactly solve the Poisson equation. The OPMC scheme has also the important advantage to be highly parallelizable due to the small number of updates of the Poisson equation needed as compared to the many-particle MC method. However, the standard OPMC method is still plagued with two important problems. Firstly, by restricting the MC simulation to only a part of the device (a so-called "window"), the current continuity between the exterior and the interior of the window is violated. This may lead to inconsistent results. Secondly, and this is also a problem of the ensemble MC method, there is no way to take the effects of generation-recombination (G-R) processes (like e.g. Shockley-Read-Hall (SRH) or impact ionisation) into account. Here, we like to insist on the term "effects". It is clear that one can compute the mean G-R rate in each point of a device also during a MC sim-

ulation, but to the authors best knowledge, no scheme has ever been proposed to compute I-V curves including G-R processes in a self-consistent way by a MC device simulation. We will present, for the first time, a general iteration scheme which keeps all advantages of the OPMC method, but solves the two problems outlined above. This scheme holds for any BTE and does not require any approximation besides those already present in the BTE itself. We will then give results for a double gate MOSFET.

2 THEORY

We found a general method and a general discretisation scheme [4],[5] that can be applied at least to any *semiconductor* BTE (linear and nonlinear) to compute moments of its inverse scattering operator S_g^{-1} with the vital property:

$$\langle S_g^{-1}|S|f \rangle = \langle g|f \rangle - \langle g|f_{eq} \rangle. \quad (1)$$

Here, S is the scattering operator (collision term in the rhs of the BTE), f_{eq} the equilibrium distribution function, and f and g are arbitrary continuous functions. Based on this theory, *exact* mobility tensors μ_{ij} and diffusion tensors D_{ij} defined as

$$\mu_{ij} := \frac{q}{n\hbar} \int_K S_{v_i}^{-1} \partial_{k_j} f d^3k, \quad (2)$$

$$D_{ij} := -\frac{1}{n} \int_K S_{v_i}^{-1} v_j f d^3k, \quad (3)$$

can be locally computed during a MC device simulation. Using these tensors, the S_v^{-1} -moment of the stationary BTE for electrons (the current equation) can be written as

$$qn\mu\vec{E} + q\nabla_r^T(n\mathbf{D}) = \vec{J}. \quad (4)$$

To solve Eq. (4) coupled with the linear Poisson equation, the continuity equation

$$-\nabla_r \cdot \vec{J} = q(G - R) \quad (5)$$

can be used. Eq. (5) is interesting, because it contains information from the MC simulation and G-R processes at the same time. Thus, solving Eq. (5) and its equivalent for holes coupled with the linear Poisson equation, a

new electric field can be computed, which contains the whole MC physics coupled with G-R processes. This new electric field can then be used for the next OPMC simulation and so on. This defines our new iterative scheme. The advantage of this scheme, besides the possibility to include G-R processes, is that the low-field transport coefficients can be used in all parts of the device where the electric field is sufficiently small. These coefficients are known and do not need to be computed during the simulation. This allows to apply the MC technique only to the regions where the Drift-Diffusion model fails without sacrificing the current continuity equation. Note that our new scheme can be easily coupled with quantum correction terms.

3 NUMERICAL METHODS

To solve Eq. (5) coupled to the Poisson equation, the finite element method (FEM) described in [4] is used.

3.1 Extraction of the Transport Coefficients

From Eqs. (2) and (3) one can see that the transport coefficients are functions of the position which can be quite complicated. In the following, all terms labeled with MC are assumed to be computed using the distribution function f^{MC} resulting from a MC simulation. To avoid the explicit computation of $\mu_{ij}^{MC}(\vec{r})$ and $D_{ij}^{MC}(\vec{r})$ (Eqs.(2) and (3)) on each element T_l of the grid (used to solve Eq.(5)), one can replace them by simpler functions $\mu_{ij}^{TM}(\vec{r})$ and $D_{ij}^{TM}(\vec{r})$ as long as the conditions

$$\int_{T_l} n^{MC}(\vec{r})\mu_{ij}^{MC}(\vec{r})d^3r = \int_{T_l} n^{MC}(\vec{r})\mu_{ij}^{TM}(\vec{r})d^3r, \quad (6)$$

and

$$\int_{T_l} \nabla_r^T(n^{MC}(\vec{r})\mathbf{D}^{MC}(\vec{r}))d^3r = \int_{T_l} \nabla_r^T(n^{MC}(\vec{r})\mathbf{D}^{TM}(\vec{r}))d^3r, \quad (7)$$

are fulfilled for all elements T_l . This is because for the FEM, only the integration of Eq. (5) with a test function is relevant.

The simplest function fulfilling Eq. (6) is a constant. Therefore, the mobility is taken as a constant 3×3 matrix on each element and is computed using the formula

$$\mu_{ij}^{TM} := \frac{q}{\hbar} \frac{\int_T \int_K S_{v_i}^{-1}(\vec{k}) \partial_{k_j} f^{MC}(\vec{r}, \vec{k}) d^3k d^3r}{\int_T n^{MC}(\vec{r}) d^3r}, \quad (8)$$

which fulfils Eq. (6). The simplest function fulfilling Eq. (7) is a linear one. The diffusivity tensor is therefore taken as a 3×3 matrix being a linear function on each element. For a triangle, it has the form

$$\mathbf{D}^{TM}(\vec{r}) = \mathbf{D}^1 \xi_1(\vec{r}) + \mathbf{D}^2 \xi_2(\vec{r}) + \mathbf{D}^3 \xi_3(\vec{r}), \quad (9)$$

where $\xi_j(\vec{r})$ is the linear function which is 1 in the point j and 0 in the others points and \mathbf{D}^1 (resp. \mathbf{D}^2 or \mathbf{D}^3) is a constant 3×3 matrix. The equivalent formula to Eq. (8) can then be found by requiring the integral of the function $n^{MC}(\vec{r})\mathbf{D}^{TM}(\vec{r})$ to be equal to the integral of the function $\int_K S_{v_i}^{-1} v_j f(\vec{r}, \vec{k}) d^3k$ on each side of the element T_l .

3.2 Iterative Scheme

Once the tensorial transport coefficients are extracted from the MC simulation, Eq.(5) can be solved using our FEM, and a new electric field can be computed. Then, a new frozen-field MC simulation is started until the transport coefficients can again be extracted. This iterative scheme may be repeated until a certain convergence criterion is achieved. In our case the criterion is that the current should fluctuate by less than 1%.

4 RESULTS

The new iteration scheme is applied to the simple double gate structure illustrated in Fig. 1. The impact ionisation (II) rate is computed during the MC simulation and Shockley-Read-Hall recombination is added via the usual model (e.g. [6]), using doping-dependent life times $\tau^{n,p}(N)$:

$$\tau^{n,p}(N) = \tau_{min}^{n,p} + \frac{\tau_{max}^{n,p} - \tau_{min}^{n,p}}{1 + \left(\frac{N}{10^{16}cm^{-3}}\right)}, \quad (10)$$

where τ^n (resp. τ^p) is the local electron (resp. hole) life time, and N is the total doping concentration. For the simulations the parameters

$$\tau_{min}^{n,p} = 0, \quad \tau_{max}^n = 10^{-5}s, \quad \tau_{max}^p = 3 \cdot 10^{-6}s, \quad (11)$$

were used.

Results are shown for a constant gate voltage (V_g) of 1.1V and for a drain bias (V_d) ranging from 0.3V to 1.3V. Fig. 1 shows the SRH recombination rate. An interesting feature is that the maximum of the SRH recombination rate is located in the source region of the device. As the device is small, the holes generated in the drain region have no time to recombine noticeably before arriving in the source region.

Figs. 2 to 5 show the effective (i.e. weighted with the associated carrier density) transport coefficients along the transport direction (x -direction, see Fig. 1).

Fig. 7 shows the effective II rate as obtained by the new method and Fig. 6 shows the hole current as a function of the drain voltage. It is noteworthy that impact ionisation starts between 0.8V and 0.9V i.e. before the drain voltage has reached the band gap energy.

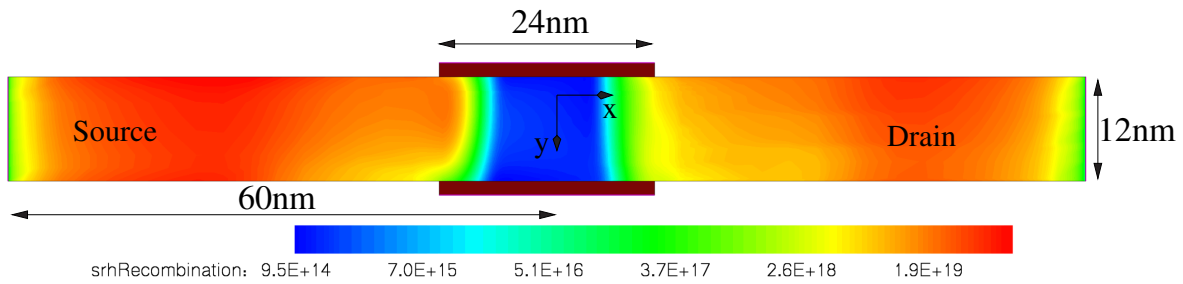


Figure 1: Double-gate MOSFET: Geometry and Shockley-Read-Hall recombination rate at $V_d = V_g = 1.1V$.

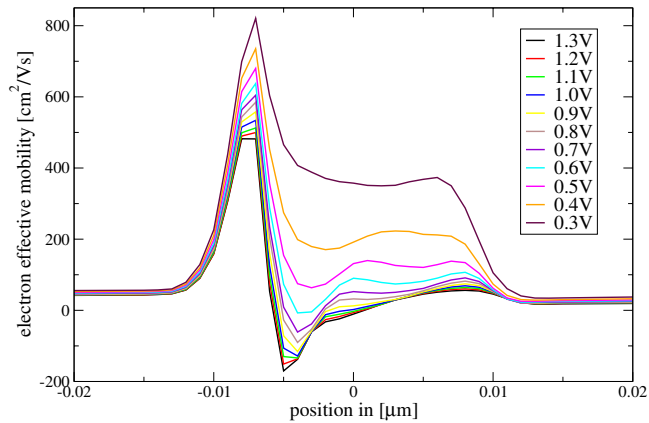


Figure 2: Profile of the xx-component of the electron effective mobility as function of the drain voltage at $V_g = 1.1V$.

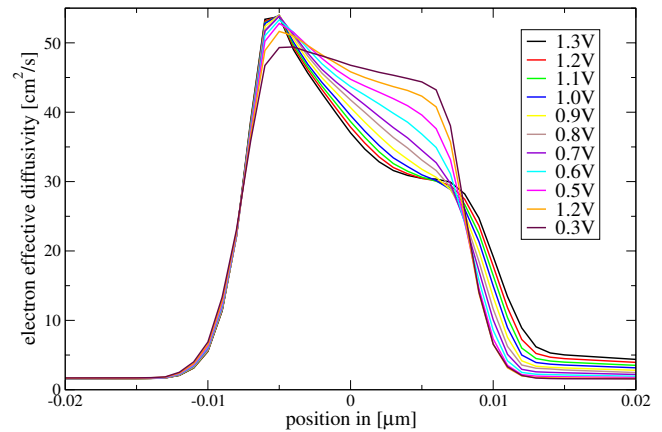


Figure 4: Profile of the xx-component of the electron effective diffusivity as function of the drain voltage at $V_g = 1.1V$.

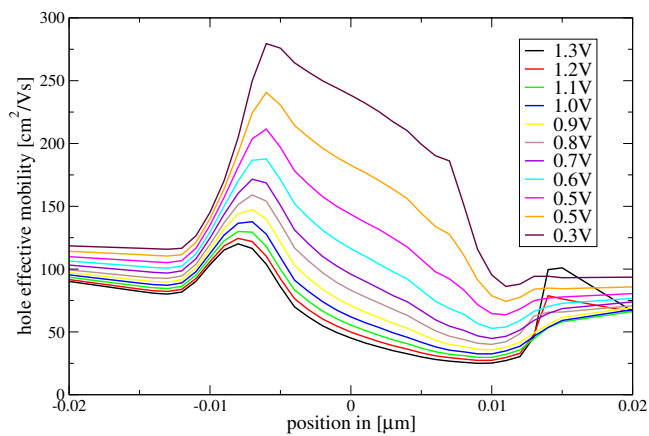


Figure 3: Profile of the xx-component of the hole effective mobility as function of the drain voltage at $V_g = 1.1V$.

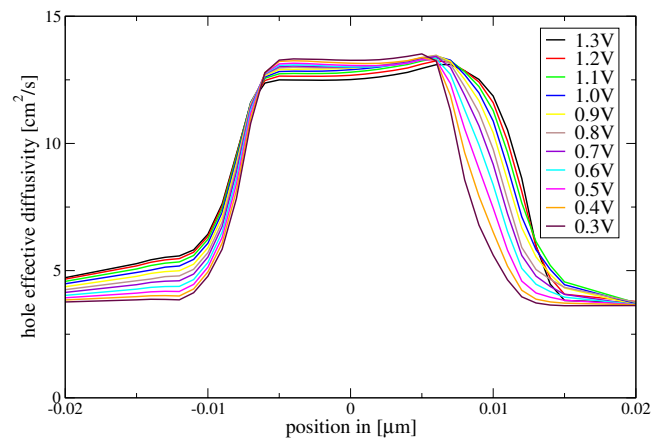


Figure 5: Profile of the xx-component of the hole effective diffusivity as function of the drain voltage at $V_g = 1.1V$.

5 CONCLUSION

A new OPMC iteration scheme has been presented to self-consistently take into account generation-recombination processes. The basic idea is to couple the BTE not only with the Poisson equation, but also with the continuity equation by using the exact transport coefficients from the MC simulation in high-field regions and the known analytical transport coefficients in low-field regions. This approach is useful e.g. for the simulation of floating-body effects in nanoscale double- and multi-gate MOSFETs. Quantum corrections as described in [7] could be easily added to this new scheme.

ACKNOWLEDGEMENT

Special thanks to the consortium of the European project SINANO (IST-2004-506844) for providing the template of the double-gate MOSFET used in this work. Financial support by Fujitsu Laboratories Ltd. and by Synopsys Switzerland LLC. is gratefully acknowledged.

REFERENCES

- [1] J. Y. Choi and J. G. Fossum. Analysis and control of floating-body bipolar effects in fully depleted sub-micrometer SOI MOSFETs. *IEEE Transactions on Electron Devices*, 38(6):1384–1391, 1991.
- [2] F. Venturi, E. C. Sangiorgi, and B. Ricco. A general-purpose device simulator coupling poisson and monte-carlo transport with application to deep sub-micron MOSFETs. *IEEE Transactions on Computer-Aided Design of Integrated Circuits and Systems*, 8(4):360–369, 1989.
- [3] F. M. Bufler, A. Schenk, and W. Fichtner. Single-particle approach to self-consistent Monte Carlo device simulation. *IEICE Transactions on Electronics*, pages 308–313, 2003.
- [4] S. C. Brugger. *Computation of Semiconductor Properties Using Moments of the Inverse Scattering Operator of the Boltzmann Equation*. PhD thesis, ETH Zürich, published at Hartung Gorre Verlag, Konstanz, 2005.
- [5] S. C. Brugger and A. Schenk. Moments of the inverse scattering operator of the Boltzmann equation: Theory and applications. *SIAM Journal on Applied Mathematics*, Accepted for publication.
- [6] W. Shockley, J. A. Copeland, and R. R. James. *Quantum Theory of Atoms, Molecules and Solid State*. Academic Press, New York, 1966.
- [7] A. Wettstein. *Quantum Effects in MOS Devices*. PhD thesis, ETH Zürich, published at Hartung Gorre Verlag, Konstanz, 2000.

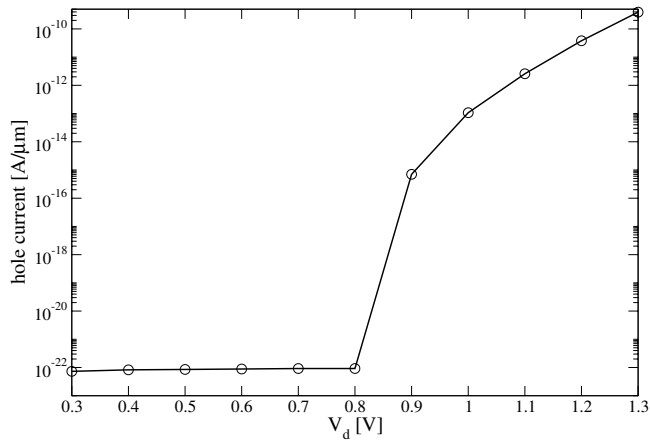


Figure 6: Hole current as function of drain voltage at $V_g = 1.1\text{V}$.

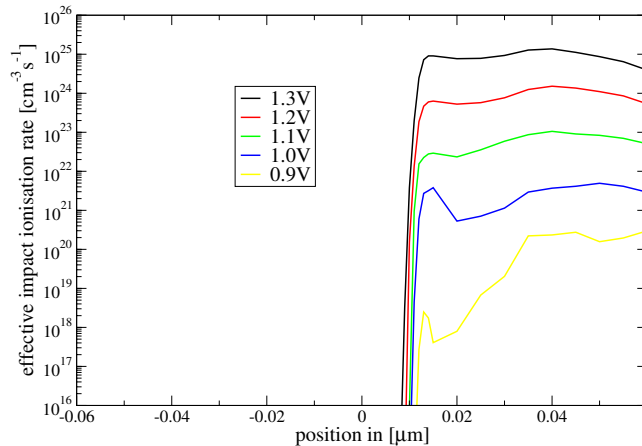


Figure 7: Profile of the effective impact ionisation rate as function of the drain voltage at $V_g = 1.1\text{V}$.